FIU-NUPAR-December 3, 2009

Large Q^2 Electrodisintegration of the Deuteron in Virtual Nucleon Approximation

Misak M. Sargsian

Florida International University,
Miami, Florida 33199, USA

Abstract

The two-body break up of the deuteron is studied at high Q^2 kinematics, with main motivation to probe the deuteron at small internucleon distances. Such studies are associated with the probing of high momentum component of the deuteron wave function. For this, two main theoretical issues have been addressed such as electromagnetic interaction of the virtual photon with the bound nucleon and the strong interaction of produced baryons in the final state of the break-up reaction. Within virtual nucleon approximation we developed a new prescription to account for the bound nucleon effects in electromagnetic interaction. The final state interaction at high Q^2 kinematics is calculated within generalized eikonal approximation (GEA). We studied the uncertainties involved in the calculation and performed comparisons with the first experimental data on deuteron electrodisintegration at large Q^2. We demonstrate that the experimental data confirm GEA's early prediction that the rescattering is maximal at $\sim 70^0$ of recoil nucleon production relative to the momentum of the virtual photon. Comparisons also show that the forward recoil nucleon angles are best suited for studies of the electromagnetic interaction of bound nucleons and the high momentum structure of the deuteron. Backward recoil angle kinematics show sizable effects due to the Δ-isobar contribution. The latter indicates the importance of further development of GEA to account for the inelastic transitions in the intermediate state of the electrodisintegration reactions.

I. INTRODUCTION

Two-body electro-disintegration of the deuteron at high Q^2 represents a powerful tool for studying one of the most fundamental issues of nuclear physics such as nuclear forces at intermediate to short distances. Despite all the successes in constructing interaction potentials for NN scattering, the most advanced potentials[1, 2, 3, 4] still use phenomenological form-factors to account for intermediate to short range interactions. Such form-factors shed little light on how nuclear forces at short distances follow from the basic concepts of QCD. Presently only the long range NN interaction is understood on fundamental QCD grounds.

The situation is not spectacular also from the experimental point of view. New experiments aimed at studies of NN interaction at short distances practically stopped after the reassignment of AGS at Brookhaven National Laboratory[66].

In this respect an alternative way of studying nuclear forces at short distances is to probe NN systems in nuclei at short space-time separations. Expectations that this can be achieved only at high-momentum transfer reactions (see e.g.[7, 8, 9, 10, 11]) was confirmed in a series of experiments with high energy electron[12, 13, 14, 15, 16] and proton probes[17, 18, 19, 20, 21]. Some of the unique results of these experiments were the observations of the scaling for the ratios of inclusive cross sections of nuclei and the deuteron[12] (or ^3He[13, 14]) at $x_{Bj} > 1$ at $Q^2 > 1.5$ GeV^2 as well as the observation of the strong (by factor of 20) dominance of pn relative to pp/nn short-range correlations in the ^{12}C nucleus for bound nucleon momenta 300-600 MeV/c[15, 16, 21]. If the first result was an indication that two (or more) nucleons can be probed at small separations, the second one was an indication of the dominance of the tensor-forces[22, 23, 24] in such correlations.

The simplest reaction which could be used to investigate short-range NN interactions using nuclear targets is the exclusive electrodisintegration of the deuteron in which large magnitudes of the relative momentum of the pn system in the ground state are probed. Three experiments[25, 26, 27] have already been performed using the relatively high (up to 6 GeV) energy electron beam of the Jefferson Lab and more comprehensive experimental program will follow after the 11 GeV upgrade of the lab[28].

The prospect of having detailed experimental data on high energy deuteron electrodisintegration makes the development of theoretical approaches for description of these reactions a pressing issue.

One of the first models for high energy break-up of the deuteron were developed in the mid 90's in which main emphasis was given to the studies of nucleon rescattering in the final state of the reactions[29, 30, 31, 32]. These models were simple in a way that they assumed a factorization of the electromagnetic γ^*N and final state NN interactions and considered the rather small values of relative momenta of the bound pn system.

The extension of these calculations to a larger internal momentum region required more elaborate approaches and several studies were done in this direction[10, 33, 34, 35, 36, 37, 38, 39].

In this work we develop a theoretical model for the description of high Q^2 exclusive electrodisintegration of the deuteron in knock-out kinematics based on virtual nucleon approximation. The main theoretical framework is based on the generalized eikonal approximation (GEA)[10, 31, 35, 40, 41, 42, 43] which allows us to represent the scattering amplitude in the covariant form using effective Feynman diagram rules. In this way all the virtualities involved in the scattering amplitudes are defined unambiguously. Reducing these amplitudes by choosing positive energy projections for the nucleon propagators allow us to represent

them through the convolutions of the deuteron wave function, on- and off- shell components of electromagnetic current and pn rescattering amplitude. In addition to accounting for the off-shell effects, nonfactorized approximation is applied to the electromagnetic and NN rescattering parts in the calculation of the final state interaction (FSI) amplitude. As a result our calculation extends beyond the distorted wave impulse approximation limit. We also estimated the charge exchange contribution in the final state interaction in addition to the $pn \to pn$ rescattering part of the FSI amplitude included in the eikonal approximation.

The paper is organized as follows. In Sec. 2 we briefly discuss the kinematics of the disintegration reaction which we consider most efficient in probing the pn system at small separations. Then we discuss the basic assumptions of virtual nuclear approximation and proceed with the derivation of scattering amplitudes and the differential cross section of the reaction.

In Sec. 3, after deriving the total scattering amplitude we performed a detailed theoretical analysis to identify the extent of uncertainties due to the off-shell part of the final state interaction as well as contribution due to charge-exchange rescattering. We also analyzed the role of the off-shell effects in the electromagnetic current of the bound nucleon. These analyses allowed us to conclude that at sufficiently large values of Q^2 (~ 6 GeV^2) the three most important contributions into the disintegration process are the off-shell electromagnetic current of the bound nucleon, the deuteron wave function and the on-shell part of the NN scattering amplitude.

Furthermore we compare our calculations with the first available high Q^2 experimental data. These comparisons allow us to confirm the early prediction of GEA that the maximal strength of FSI corresponds to $\sim 70^0$ production of the recoil nucleon relative to the direction of the virtual photon. We also found that forward angles of recoil nucleon are best suited for studies of the off-shell electromagnetic current and the deuteron wave function. Another observation is that in backward direction there is a sizable contribution due to the Δ-Isobar production at the intermediate state of the reaction. In Sec. 4 we give conclusions and an outlook on further development of the model.

II. CROSS SECTION OF THE REACTION

A. Kinematics

We discuss the process:

$$e + d \to e' + p + n, \tag{1}$$

in knock-out kinematics in which case one nucleon (for definiteness we consider it to be a proton) absorbs the virtual photon and carries almost all its momentum. The optimal kinematics for probing the initial pn system at close distances is defined as follows:

$$\text{(a) } Q^2 \geq 1 \text{ GeV}^2; \quad \text{(b) } \vec{p}_f \approx \vec{q}; \quad \text{(c) } \; p_f \gg p_r \geq 300 \text{ MeV/c}, \tag{2}$$

where we define $q \equiv (q_0, \vec{q})$, $p_f \equiv (E_f, \vec{p}_f)$ and $p_r = (E_r, \vec{p}_r)$ as four-momenta of virtual photon, knock-out proton and recoil neutron respectively. Also $Q^2 = |\vec{q}|^2 - q_0^2$. Conditions (2)(b) and (c) define the knock-out process, while condition (2)(a) is necessary to satisfy Eq.(2)(c). From the point of view of the dynamics of the reaction one also needs Eq.(2)(a) in order to provide a necessary resolution for probing the deuteron at small inter-nucleon distances.

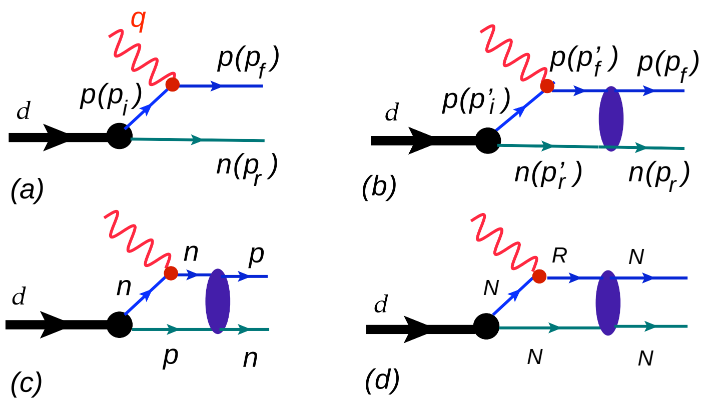

FIG. 1: GEA diagrams

In the most simple picture the kinematics of Eq.(2) represent a scenario in which the high energy virtual photon removes the proton from the pn system leaving the neutron with the pre-existing relative momentum p_r (see Fig.(1)a).

B. Main Assumptions of Virtual Nucleon Approximation

The virtual nucleon approximation is based on the following main assumptions which also define the limits of its validity. First, one considers only the pn component of the deuteron, neglecting inelastic initial state transitions. Since the deuteron is in a isosinglet state this will correspond to restricting the kinetic energy of recoil nucleon to

$$T_N < 2(m_\Delta - m_N) \sim (m_{N^*} - m) \sim 500 \text{ MeV} \quad (3)$$

where m, m_Δ and m_{N^*} are masses of the nucleon and low-lying non-strange baryonic resonances, $\Delta(1232)$ and $N^*(1525)$. We neglect also the pionic degrees of freedom in the deuteron wave function. However we expect that the overall error introduced by this approximation to be small since the probability of low momentum pionic degrees of freedom is suppressed due to pseudogoldstone nature of pions in QCD as well as observation that πNN form factors are soft (see e.g. discussion in Refs.[8, 11]).

The second assumption is that the negative energy projection of the virtual nucleon propagator gives negligible contribution to the scattering amplitude. Such an assumption can be justified if,

$$M_d - \sqrt{m^2 + p^2} > 0, \quad (4)$$

where M_d is the mass of the deuteron and p is the relative momentum of the bound pn system.

The above two conditions can be satisfied if we restrict the momentum of the recoil neutron, $p_r \leq 700$ MeV/c. However due to the fact that we explicitly left out the non-nucleonic components of deuteron wave function, the momentum sum rule is not satisfied in virtual nucleon approximation (see discussions in Refs.([8, 59, 60]).

The third assumption which is made in the calculations is that at large Q^2 (> 1 GeV^2) the interaction of virtual photon with exchanged mesons are a small correction and can be neglected (see e.g. discussions in Ref.[9, 10]).

C. Generalized Eikonal Approximation

The assumptions discussed above allow us to restrict the consideration by the set of Feynman diagrams presented in Fig.(1). One can calculate these diagrams based on the effective Feynman diagram rules discussed in Ref.[10]. These rules allow us to formulate scattering amplitudes in the covariant form which unambiguously accounts for all the off-shell effects. Then we reduce the covariant amplitudes into a non-covariant form by choosing the positive energy projection of nucleon (or baryonic resonance) propagators at the intermediate state of the reaction.

Fig.1(a) diagram corresponds to the plane wave impulse approximation (PWIA) in which the virtual photon knocks out one of the nucleons from the deuteron leaving the second nucleon in the on-shell positive energy state. Two nucleons do not interact in the final state of the reaction representing two outgoing plane waves. The diagram of Fig.1(b) represents a situation in which the elastic electroproduction is followed by the elastic $pn \to pn$ rescattering. In this case the rescattering is forward in the sense that, for example, the proton struck by the virtual photon will attain its large momentum after the $pn \to pn$ rescattering. The amplitude of this scattering will be referred to as a forward FSI amplitude.

The diagram of Fig1(c) corresponds to the scenario in which final state interaction proceeds through the charge-exchange $pn \to np$ rescattering. In this case the final fast proton emerges from the process in which the photon strikes the neutron which then undergoes a $np \to pn$ charge-exchange rescattering. The amplitude of this scattering process will be referred to as a charge-exchange FSI amplitude.

The fourth diagram (Fig.1(d)) corresponds to the electroproduction of an excited state R with a subsequent $RN \to NN$ final state rescattering. The most important contribution to the fourth diagram is due to the Δ-isobar (IC), whose production threshold is closest to the quasielastic scattering kinematics. Several factors make IC contribution small in high Q^2 limit at $x \geq 1$[9, 10]. One factor is the large longitudinal momenta of the initial nucleon involved in the Δ-electroproduction process:

$$p_{i,z}^{IC} = (1-x)m - \frac{m_\Delta^2 - m^2}{2q}, \tag{5}$$

which indicates that choosing $x > 1$ one can suppress the electroproduction of Δ-resonance in the intermediate states due to the large values of initial momenta entering in the deuteron wave function.

An additional suppression of IC follows from the smallness of the $\gamma^* N \to \Delta$ transition form-factors as compared to the elastic form factors at $Q^2 \geq few$ GeV^2[49, 50]. Finally, due to the fact that the $\Delta N \to NN$ amplitude is dominated by pion or ρ-type reggeon exchanges, it will be additionally suppressed by at least the factor of $\frac{1}{\sqrt{Q^2}}$. In any case this contribution can be calculated in a selfconsistent way within the generalized eikonal approximation. The calculation of these types of diagrams within GEA will be presented elsewhere[44].

Below we will discuss the calculations of only the first three diagrams of Fig.1.

1. *Plane Wave Impulse Approximation Amplitude*

The amplitude of the PWIA diagram in the covariant form can be written as follows:

$$\langle s_f, s_r \mid A_0^\mu \mid s_d\rangle = -\bar{u}(p_r, s_r)\Gamma^\mu_{\gamma^* p}\frac{\not{p}_i + m}{p_i^2 - m^2} \cdot \bar{u}(p_f, s_f)\Gamma_{DNN} \cdot \chi^{s_d}, \tag{6}$$

where $\Gamma_{\gamma^* p}$ is the electromagnetic vertex of the $\gamma^* N \to N$ scattering and the vertex function Γ_{DNN} describes the transition of the deuteron into the pn system. The notations s_d, s_f, s_r describe the spin projections of the deuteron, knock-out proton and recoil neutron respectively. The spin function of the deuteron is represented by χ^{s_d}. The four-momentum of the struck nucleon in the initial state within PWIA is defined as:

$$p_i = (E_d - E_r, \vec{p}_d - \vec{p}_r) = (M_d - E_r, -\vec{p}_r) \mid_{LaB} . \tag{7}$$

The above relation clearly shows the off-shell character of the struck nucleon in the initial state, since $p_i^2 \neq m^2$. Therefore expressing the initial nucleon's propagator through the on-mass shell nucleonic spinors is not valid.

However, using an approximation in which only positive energy projections are taken into account, one can isolate the on-shell part of the propagator by adding and subtracting $E_i^{on}\gamma^0$ term to $\not{p}_i$ as follows:

$$\not{p}_i + m = \not{p}_i^{on} + m + (E_i^{off} - E_i^{on})\gamma^0, \tag{8}$$

where $E_i^{off} = M_d - \sqrt{m_n^2 + p_r^2}$ and $E_i^{on} = \sqrt{m_p + p_r^2}$ where m_n and m_p are the masses of the proton and neutron respectively[67]. Now we can separate the PWIA amplitude into on- and off-shell parts in the following way:

$$\langle s_f, s_r \mid A_0^\mu \mid s_d\rangle = \langle s_f, s_r \mid A_{0,on}^\mu \mid s_d\rangle + \langle s_f, s_r \mid A_{0_{off}}^\mu \mid s_d\rangle, \tag{9}$$

where

$$\langle s_f, s_r \mid A_{0,on}^\mu \mid s_d\rangle = -\bar{u}(p_r, s_r)\Gamma^\mu_{\gamma^* p}\frac{\not{p}_i^{on} + m}{p_i^2 - m^2} \cdot \bar{u}(p_f, s_f)\Gamma_{DNN}\chi_d^s, \tag{10}$$

and

$$\langle s_f, s_r \mid A_{0,off}^\mu \mid s_d\rangle = -\bar{u}(p_r, s_r)\Gamma^\mu_{\gamma^* p}\frac{(E_i^{off} - E_i^{on})\gamma^0}{p_i^2 - m^2} \cdot \bar{u}(p_f, s_f)\Gamma_{DNN}\chi_d^s. \tag{11}$$

For the on-shell part of the amplitude, using

$$\not{p}_i^{on} + m = \sum_{s_i} u(p_i, s_i)\bar{u}(p_i, s_i) \tag{12}$$

and the definition[45, 46],

$$\Psi_d^{s_d}(s_1, p_1, s_2, p_2) = -\frac{\bar{u}(p_1, s_1)\bar{u}(p_2, s_2)\Gamma_{DNN}^{s_d}\chi_{s_d}}{(p_1^2 - m^2)\sqrt{2}\sqrt{(2\pi)^3(p_2^2 + m^2)^{\frac{1}{2}}}} \tag{13}$$

one obtains

$$\langle s_f, s_r \mid A_{0,on}^\mu \mid s_d\rangle = \sqrt{2}\sqrt{(2\pi)^3 2E_r}\sum_{s_i} J_{N,on}^\mu(s_f, p_f; s_i, p_i)\Psi_d^{s_d}(s_i, p_i, s_r, p_r), \tag{14}$$

where

$$J^{\mu}_{N,on}(s_f,p_f;s_i,p_i) = \bar{u}(p_f,s_f)\Gamma^{\mu}_{\gamma^*N}u(p_i,s_i). \tag{15}$$

For the off-shell part of the scattering amplitude one observes that the following relation,

$$\bar{u}(p_2,s_2)\Gamma_{DNN}\chi^{s_d} = -\sum_{s_1}\frac{u(p_1,s_1)\Psi^{s_d}_d(s_1,p_1,s_2,p_2)}{2m}(p_1^2-m^2)\sqrt{2}\sqrt{(2\pi)^3 2(p_1^2+m^2)^{\frac{1}{2}}} \tag{16}$$

satisfies Eq.(13). Inserting it into Eq.(11) one obtains

$$\langle s_f,s_r \mid A^{\mu}_{0,off} \mid s_d\rangle = \sqrt{2}\sqrt{(2\pi)^3 2E_r}\sum_{s_i} J^{\mu}_{N,off}(s_f,p_f;s_i,p_i)\Psi^{s_d}_d(s_i,p_i,s_r,p_r), \tag{17}$$

where

$$J^{\mu}_{N,off}(s_f,p_f;s_i,p_i) = \bar{u}(p_f,s_f)\Gamma^{\mu}_{\gamma^*N}\gamma^0 u(p_i,s_i)\frac{E^{off}_i - E^{on}_i}{2m}, \tag{18}$$

and $E^{off}_i = M_d - E^{on}_i$ and $E^{on}_i = \sqrt{m^2+p_i^2}$.

One can combine on-and off-shell parts of the PWIA scattering amplitudes in the following form:

$$\langle s_f,s_r \mid A^{\mu}_{0} \mid s_d\rangle = \sqrt{2}\sqrt{(2\pi)^3 2E_r}\sum_{s_i} J^{\mu}_{N}(s_f,p_f;s_i,p_i)\Psi^{s_d}_d(s_i,p_i,s_r,p_r), \tag{19}$$

where

$$J^{\mu}_{N}(s_f,p_f;s_i,p_i) = J^{\mu}_{N,on}(s_f,p_f;s_i,p_i) + J^{\mu}_{N,off}(s_f,p_f;s_i,p_i). \tag{20}$$

The above form of the electromagnetic current together with Eqs.(15) and (18) represents our off-shell approximation. It is worth noting that the first, "on-shell" part of this current corresponds to the widely used "De Forest" approximation[47]. In the "DeForest" approximation because of the absence of the second term the gauge invariance is violated and the current conservation is restored by expressing J_0 or J_z components through each other with different assumptions for the nucleon spinors and electromagnetic vertices. The latter introduces more uncertainty since imposed relations are not unique. As a result one generates several forms of the off-shell electromagnetic currents[47].

The additional "off-shell" part of the electromagnetic current in Eq.(20) obtained in our approximation reduces the uncertainty of choosing on-shell nucleon spinors which is inherent to the "De Forest" approximation. The total current in Eq.(20) is conserved since it is derived from the gauge invariant amplitude of Eq.(6). Therefore our approximation does not violate gauge invariance and no additional conditions are needed to restore the current conservation.

Note that our approximation is analogous to the one used in hadronic physics within light-cone approximation (see e.g. [48]) in which case an off-shell "γ^+" component of the fermion propagator is isolated in the similar manner as it is done for the γ^0 component in our case.

2. *Forward Elastic Final State Interaction Amplitude*

We start by applying effective Feynman diagram rules to the diagram of Fig.(1)b, which yields:

$$\langle s_f,s_r \mid A^{\mu}_{1} \mid s_d\rangle \;=\; -\int\frac{d^4p'_r}{i(2\pi)^4}\frac{\bar{u}(p_f,s_f)\bar{u}(p_r,s_r)F_{NN}[\not{p}'_r+m][\not{p}_d-\not{p}'_r+\not{q}+m]}{(p_d-p'_r+q)^2-m^2+i\epsilon}$$

$$\times \frac{\Gamma_{\gamma^* N}[\not p_d - \not p'_r + m]\Gamma_{DNN}\chi^{s_d}}{((p_d - p'_r)^2 - m^2 + i\epsilon)(p'^2_r - m^2 + i\epsilon)}, \tag{21}$$

were F_{NN} represents the invariant $pn \to pn$ scattering amplitude that can be expressed as follows:

$$F_{NN}(s,t) = \sqrt{s(s-4m^2)} f_{NN}(s,t) \tag{22}$$

where s is the total invariant energy of the scattering pn system and the f_{NN} scattering amplitude is defined in such a way that $Im f_{NN} = \sigma_{tot}$. Furthermore we will use the following four-vectors defined as

$$p'_i = p_d - p'_r \ \text{ and } \ p'_f = p_d - p'_r + q. \tag{23}$$

We first integrate by $d^0 p'_r$ through the positive energy pole of the spectator nucleon propagator at the intermediate state;

$$\int \frac{d^0 p'_r}{p'^2_r - m^2 + i\epsilon} = -i \frac{2\pi}{2E'_r}. \tag{24}$$

This integration allows us to use $\not p'_r + m = \sum\limits_{s'_r} u(p'_r, s'_r)\bar{u}(p'_r, s'_r)$. For $\not p_d - \not p'$ we use a relation similar to Eq.(8). The same could be done for $\not p_d - \not p'_r + \not q$. However for large values of q the off-shell part in Eq.(8) is suppressed by $\frac{|\vec{q}| - q_0}{|\vec{q}|}$ and in large Q^2 limit it's contribution is negligible. Thus we can use the on-shell relation, $\not p_d - \not p' + \not q = \sum\limits_{s'_f} u(p'_f, s'_f)\bar{u}(p'_f, s'_f)$ for the knock-out nucleon spinors in the intermediate state. Using the above representations of the spinors, the definitions of the deuteron wave function (Eq.(13)) and electromagnetic current (Eq.(20)) for the scattering amplitude of Eq.(21) we obtain:

$$\langle s_f, s_r \mid A_1^\mu \mid s_d \rangle = -\sqrt{2}(2\pi)^{\frac{3}{2}} \sum_{s'_f, s'_r, s_i} \int \frac{d^3 p'_r}{i(2\pi)^3} \frac{\sqrt{2E'_r}\sqrt{s(s-4m^2)}}{2E'_r((p_d - p'_r + q)^2 - m^2 + i\epsilon)} \times$$
$$\langle p_f, s_f; p_r, s_r \mid f^{NN}(t,s) \mid p'_r, s'_r; p'_f, s'_f \rangle \cdot J_N^\mu(s'_f, p'_f; s_i, p_i) \cdot \Psi_d^{s_d}(s_i, p'_i, s'_r, p'_r). \tag{25}$$

Next, we consider the propagator of the knock-out proton in the intermediate state, using the condition of quasielastic scattering

$$(q + p_d - p_r)^2 = p_f^2 = m^2, \tag{26}$$

one obtains

$$(p_d - p'_r + q)^2 - m^2 + i\epsilon = 2|\mathbf{q}|(p'_{r,z} - p_{r,z} + \Delta + i\epsilon), \tag{27}$$

where

$$\Delta = \frac{q_0}{|\mathbf{q}|}(E_r - E'_r) + \frac{M_d}{|\mathbf{q}|}(E_r - E'_r) + \frac{p'^2_r - m^2}{2|\mathbf{q}|}. \tag{28}$$

Furthermore using the relation

$$\frac{1}{(p'_{r,z} - p_{r,z} + \Delta + i\epsilon} = -i\pi\delta(p'_{r,z} - (p_{r,z} - \Delta)) + \mathcal{P}\int \frac{1}{p'_{r,z} - (p_{r,z} - \Delta)} \tag{29}$$

and performing integration over $p'_{r,z}$ we split the scattering amplitude into two terms; one containing on-shell and the other off-shell $pn \to pn$ scattering amplitudes as follows:

$$\langle s_f, s_r \mid A_1^\mu \mid s_d\rangle = \frac{i\sqrt{2}(2\pi)^{\frac{3}{2}}}{4} \sum_{s'_f, s'_r, s_i} \int \frac{d^2 p'_r}{(2\pi)^2} \frac{\sqrt{2\tilde{E}'_r}\sqrt{s(s-4m^2)}}{2\tilde{E}'_r |q|} \times$$
$$\langle p_f, s_f; p_r, s_r \mid f^{NN,on}(t,s) \mid \tilde{p}'_r, s'_r; \tilde{p}'_f, s'_f\rangle \cdot J_N^\mu(s'_f, p'_f; s_i, \tilde{p}'_i) \cdot \Psi_d^{s_d}(s_i, \tilde{p}'_i, s'_r, \tilde{p}'_r)$$
$$-\frac{\sqrt{2}(2\pi)^{\frac{3}{2}}}{2} \sum_{s'_f, s'_r, s_i} \mathcal{P} \int \frac{dp'_{r,z}}{2\pi} \int \frac{d^2 p'_r}{(2\pi)^2} \frac{\sqrt{2E'_r}\sqrt{s(s-4m^2)}}{2E'_r |\mathbf{q}|} \times$$
$$\frac{\langle p_f, s_f; p_r, s_r \mid f^{NN,off}(t,s) \mid p'_r, s'_r; p'_f, s'_f\rangle}{p'_{r,z} - \tilde{p}'_{r,z}} J_N^\mu(s'_f, p'_f; s_i, p'_i) \cdot \Psi_d^{s_d}(s_i, p'_i, s'_r, p'_r), \quad (30)$$

where $\tilde{p}'_r = (p_{r,z} - \Delta, p'_{r,\perp})$, $\tilde{E}'_r = \sqrt{m^2 + \tilde{p}'^2_r}$, $\tilde{p}'_i = p_d - \tilde{p}'_r$ and $\tilde{p}'_f = \tilde{p}'_i + q$.

For numerical estimates of the above amplitudes one needs on- and off-shell $pn \to pn$ amplitudes as an input. In high energy limit in which the helicity conservation of small angle NN scattering is rather well established the on-shell amplitude is predominantly imaginary and can be parameterized in the form

$$\langle p_f, s_f; p_r, s_r \mid f^{NN,on}(t,s) \mid \tilde{p}'_r, s'_r; \tilde{p}'_f, s'_f\rangle = \sigma_{tot}^{pn}(i+\alpha) e^{\frac{B}{2}t} \delta_{s_f, s'_f} \delta_{s_r, s'_r}, \quad (31)$$

where $\sigma_{tot}^{pn}(s)$, $B(s)$ and $\alpha(s)$ are found from fitting of experimental data on elastic $pn \to pn$ scattering. For the effective lab momentum range of up to 1.3 GeV/c the SAID parameterization[51] of pn amplitudes can be used. The situation is more uncertain for the half-off-shell part of the $f^{NN,off}$ amplitude. In present calculations we use the following parameterization:

$$f^{NN,off} = f^{NN,on} e^{B(m_{off}^2 - m^2)}, \quad (32)$$

where $m_{off}^2 = (M_d - E'_r + q_0)^2 - (p'_r + q)^2$. Overall we expect that our calculation will not be reliable in situations in which the contribution from the off-shell part of the rescattering is dominant. However in high Q^2 limit this contribution is only a small correction.

Completing this section it is worth to notice that in addition to the appearance of the Δ factor (Eq.(28)) in GEA which does not enter in conventional Glauber approximation (see detailed discussion in Ref.[10]), the new factor, $\frac{\sqrt{s(s-4m^2)}}{2E'_r|q|}$ entering the elastic FSI amplitude (Eq.(30)) is also unique to GEA. Within conventional Glauber approximation, in which Fermi motion of the scatterers is neglected this factor is equal to one. However within GEA it appears as a consequence of the covariant form of the initial scattering amplitude. Calculation of this factors for our kinematics yields:

$$\frac{\sqrt{s(s-4m^2)}}{2E'_r|q|} = \frac{\sqrt{(\frac{2-x}{x}Q^2 - m_D^2)(\frac{2-x}{x}Q^2)}}{2E'_r|q|} \quad (33)$$

which decreases with $x \to 2$. Thus for the $x > 1$ and large Q^2 kinematics GEA predicts an additional suppression of FSI as compared to the conventional Glauber approximation.

3. Charge-Exchange Final State Interaction Amplitude

To complete the calculation of the total amplitude we need to include the contribution from charge-exchange rescattering, which can be obtained from Eq.(30) after the substitutions corresponding to Fig.1c. Namely, one needs to switch the proton and neutron lines in the initial and intermediate states of the scattering, replace proton electromagnetic current by the neutron and f_{NN} by the charge-exchange scattering amplitude f^{chex}_{NN}. One obtains:

$$\langle s_f, s_r \mid A^{\mu}_{1,chex} \mid s_d\rangle = \frac{i\sqrt{2}(2\pi)^{\frac{3}{2}}}{4} \sum_{s'_f,s'_r,s_i} \int \frac{d^2p'_r}{(2\pi)^2} \frac{\sqrt{2\tilde{E}'_r}\sqrt{s(s-4m^2)}}{2\tilde{E}'_r|q|} \times$$
$$\langle p_f, s_f; p_r, s_r \mid f^{chex,on}(t,s) \mid \tilde{p}'_r, s'_r; \tilde{p}'_f, s'_f\rangle \cdot J^{\mu}_n(s'_f, p'_f; s_i, \tilde{p}'_i) \cdot \Psi^{s_d}_d(s_i, \tilde{p}'_i, s'_r, \tilde{p}'_r)$$
$$-\frac{\sqrt{2}(2\pi)^{\frac{3}{2}}}{2} \sum_{s'_f,s'_r,s_1} \mathcal{P}\int \frac{dp'_{r,z}}{2\pi} \int \frac{d^2p'_r}{(2\pi)^2} \frac{\sqrt{2E'_r}\sqrt{s(s-4m^2)}}{2E'_r|\mathbf{q}|} \times$$
$$\frac{\langle p_f, s_f; p_r, s_r \mid f^{chex,off}(t,s) \mid p'_r, s'_r; p'_f, s'_f\rangle}{p'_{r,z} - \tilde{p}'_{r,z}} J^{\mu}_n(s'_f, p'_f; s_i, p'_i) \cdot \Psi^{s_d}_d(s_i, p'_i, s'_r, p'_r). \quad (34)$$

Here the charge-exchange rescattering amplitude f^{chex}_{NN}, similar to the elastic FSI case is taken from the experimental measurements. The off-shell extrapolation of the rescattering amplitude is also done similar to Eq.(32). For numerical estimates we use the parameterization of Ref.[61].

4. Deuteron Wave Function

The deuteron wave function in Eq.(13) in general represents a solution of the Bethe-Salpeter type equation. To fix the normalization of the wave function we need to relate an expression that contains the deuteron wave function (as it is defined in Eq.(13)) to a well defined quantity characterizing the deuteron. One such quantity is the deuteron elastic charge form-factor G_C, which at $Q^2 \to 0$ limit approaches to one, i.e. $G_C(Q^2 = 0) = 1$ (see e.g. Ref.[53]). The latter could be related to the deutron elastic scattering amplitude as follows:

$$\frac{1}{4M_d} \sum_{s'_d=s_d=-1}^{1} \langle p'_d, s'_d \mid A^{\mu=0}(Q^2) \mid p_d, s_d\rangle \mid_{Q^2\to 0} = G_C(0) = 1, \quad (35)$$

where $\langle p'_d, s'_d \mid A^{\mu} \mid p_d, s_d\rangle$ is the elastic $\gamma^* d \to d'$ scattering amplitude corresponding to the diagram of Fig.2.

Applying the same effective Feynman diagram rules used above for $\langle p'_d, s'_d \mid A^{\mu} \mid p_d, s_d\rangle$ one obtains:

$$\langle p'_d, s'_d \mid A^{\mu} \mid p_d, s_d\rangle = -\sum_{p,n} \int \frac{d^4p_r}{i(2\pi)^4} \chi^{s'_d,\dagger}\Gamma^{\dagger}_{DNN} \frac{\not{p}_2 + m}{p_2^2 - m^2 + i\epsilon} \Gamma^{\mu}_{\gamma^* N} \frac{\not{p}_1 + m}{p_1^2 - m^2 + i\epsilon} \Gamma_{DNN} \chi^{s_d}$$
$$\times \frac{\not{p}_r + m}{p_r^2 - m^2 + i\epsilon}. \quad (36)$$

Further derivations within the virtual nucleon approximation follow the similar to Secs.II.C.1 and II.C.2 steps. We first evaluate dp^0_r integral by the pole value of the spectator

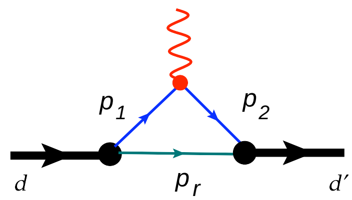

FIG. 2: Elastic $\gamma^* d \to d'$ diagram.

nucleon propagator, then separate the on- and off-shell parts in the numerator of interacting nucleon propagators and introduce deuteron wave function according to Eq.(13). In this case the electromagnetic current of the nucleon is fully off-shell since the struck nucleon is bound in both initial and final states of the reaction. This results in the following expression for the elastic scattering amplitude:

$$\langle p'_d, s'_d \mid A^\mu \mid p_d, s_d\rangle = 4\sum_{p,n}\sum_{s_2,s_1,s_r}\int d^3p_r \Psi_d^{s'_d\dagger}(s_2,p_2,s_r,p_r)\bar{u}(p_2,s_2)\left[I + \frac{E_2^{off}-E_2^{on}}{2m}\gamma_0\right] \Gamma^\mu_{\gamma^* N}\left[I + \frac{E_1^{off}-E_1^{on}}{2m}\gamma_0\right] u(p_1,s_1)\Psi_d^{s_d}(s_1,p_1,s_r,p_r). \quad (37)$$

Neglecting the second order off-shell terms in the above equation (i.e. $(\frac{E^{off}-E^{on}}{2m})^2$) one obtains:

$$\langle p'_d, s'_d \mid A^\mu \mid p_d, s_d\rangle = 4\sum_{p,n}\sum_{s_2,s_1,s_r}\int d^3p_r \Psi_d^{s'_d\dagger}(s_2,p_2,s_r,p_r)\tilde{J}^\mu_N \Psi_d^{s_d}(s_1,p_1,s_r,p_r), \quad (38)$$

where

$$\tilde{J}^\mu_N(s_2,p_2;s_1,p_1) = J^\mu_{N,on}(s_2,p_2;s_1,p_1) + J^\mu_{N,off}(s_2,p_2^{off};s_1,p_1) + J^\mu_{N,off}(s_2,p_2;s_1,p_1^{off}). \quad (39)$$

Here the on- and off- shell parts of electromagnetic current are defined in Eq.(15) and (18). In the above equation the notation p^{off} in the argument of $J_{N,off}$ indicates which nucleon is considered as off-shell.

Using now the fact that for the proton and neutron $F_{1p(n)}(Q^2=0) = 1(0)$ and using Eqs.(15,18) one obtains:

$$\begin{aligned} \tilde{J}_p^{\mu=0}\mid_{Q^2\to 0} &= 2E_1^{off} \\ \tilde{J}_p^{\mu=0}\mid_{Q^2\to 0} &= 0. \end{aligned} \quad (40)$$

Using these relations and inserting Eq.(38) into Eq.(35) one obtains

$$\sum_{s_d=-1}^{1}\int \mid \Psi_d^{s_d}(p)\mid^2 \frac{2E_{off}}{M_d} d^3p = 1 \quad (41)$$

where $E^{off} = M_d - \sqrt{m^2+p^2}$. It is worth mentioning that above normalization coincides with the normalization obtained from the baryon number conservation sum rule[54, 55, 56, 57, 58, 59, 60] for deep inelastic scattering off the deuteron:

$$\int |\Psi_d(\alpha,p_t)|^2 \alpha d^3p = 1 \quad (42)$$

where $\alpha = \frac{M_d - \sqrt{m^2+p^2} - p_z}{m}$ is the light-cone momentum fraction of the deuteron carried by the struck nucleon. As it was mentioned in Sec.II.B in virtual nucleon approximation due to unaccounted non-nucleonic degrees of freedom the wave function defined according to Eq.(13) will not satisfy the energy-momentum sum rule which expresses the requirement that the sum of the light-cone momentum fractions of all the constituents of the nucleus equals to one.

For numerical estimates we model the deuteron wave function to satisfy Eq.(41) in the following form[56, 60]:

$$\Psi_d(p) = \Psi_d^{NR}(p)\frac{M_d}{2(M_d - \sqrt{m^2+p^2})} \tag{43}$$

which provides a smooth transition to the nonrelativistic wave function Ψ^{NR} in the small momentum limit.

5. *Total amplitude and the differential cross section*

The total scattering amplitude consists of the sum of PWIA, forward and charge-exchange FSI amplitudes:

$$\langle s_f, s_r \mid A^\mu \mid s_d\rangle = \langle s_f, s_r \mid A_0^\mu \mid s_d\rangle + \langle s_f, s_r \mid A_1^\mu \mid s_d\rangle + \langle s_f, s_r \mid A_{1,chex}^\mu \mid s_d\rangle. \tag{44}$$

Using this amplitude the differential cross section is calculated as follows:

$$\frac{d\sigma}{dE'_e, d\Omega_{e'} dp_f d\Omega_f} = \frac{\alpha^2 E'_e}{q^4 E_e}\cdot\frac{1}{6}\sum_{s_f,s_r,s_d,s_1,s_2}\frac{\mid J_e^\mu J_{d,\mu}\mid^2}{2M_d E_f}\frac{p_f^2}{\mid \frac{p_f}{E_f} + \frac{p_f - q cos(\theta_{p_f,q})}{E_r}\mid} \tag{45}$$

where

$$J_e^\mu = \bar{u}(k_2, s_2)\gamma^\mu u(k_1, s_1) \tag{46}$$

and

$$J_d^\mu = \frac{\langle s_f, s_r \mid A^\mu \mid s_d\rangle}{\sqrt{2(2\pi)^3 2E_r}}. \tag{47}$$

For numerical estimates we use the electromagnetic current of the nucleon in the form

$$\Gamma^\mu = F_1(Q^2)\gamma^\mu + \frac{F_2(Q^2)}{2m} i\sigma^{\mu,\nu}q_\nu, \tag{48}$$

where F_1 and F_2 are Dirac form-factors and for their evaluation the available phenomenological parameterizations are used[52]. For the deuteron wave function we use the approximation of Eq.(43) with the non-relativistic wave function calculated based on the Paris potential[4]. The pn scattering amplitude is parameterized in the form of Eq.(31) and its off-shell extrapolation in the form of Eq.(32). Also, for f_{pn} in the lower momentum range ($p_{lab} \leq 1.3$ GeV/c) we use the SAID parameterization[51] based on the pn scattering phase-shifts.

III. OBSERVABLES

The main quantity which we will consider for numerical estimates is the ratio of the calculated cross section which includes total amplitude of Eq.(44) to the cross section calculated within PWIA:

$$R = \frac{\sigma}{\sigma^{PWIA}} \tag{49}$$

where $\sigma \equiv= \frac{d\sigma}{dE'_e, d\Omega_{e'} dp_f d\Omega_f}$. This ratio allows us to clearly distinguish between kinematics in which PWIA dominates $R \approx 1$ from kinematics in which FSI is dominated by screening $R < 1$ or single rescattering $R > 1$ effects (see e.g. [31, 40, 62]).

Considering the numerical estimates of the ratio R we will discuss four main effects which characterize our present theoretical approach. These are the unfactorization of the electromagnetic interaction in the FSI amplitude, the off-shell effects in the final state interaction, the effects of charge-exchange rescatterings and the off-shell effects in the electromagnetic interaction of the bound nucleon.

In our estimates we will study the dependence of R on the angle of the recoil neutron relative to $\vec{q}$ for different values of neutron momenta. We will perform our calculations for two values of Q^2 (2 GeV^2 and 6 GeV^2) which will allow us to also assess the Q^2 dependence of the considered effects.

Finally, we will present the comparisons with the first experimental data on the deuteron electrodisintegration at large Q^2.

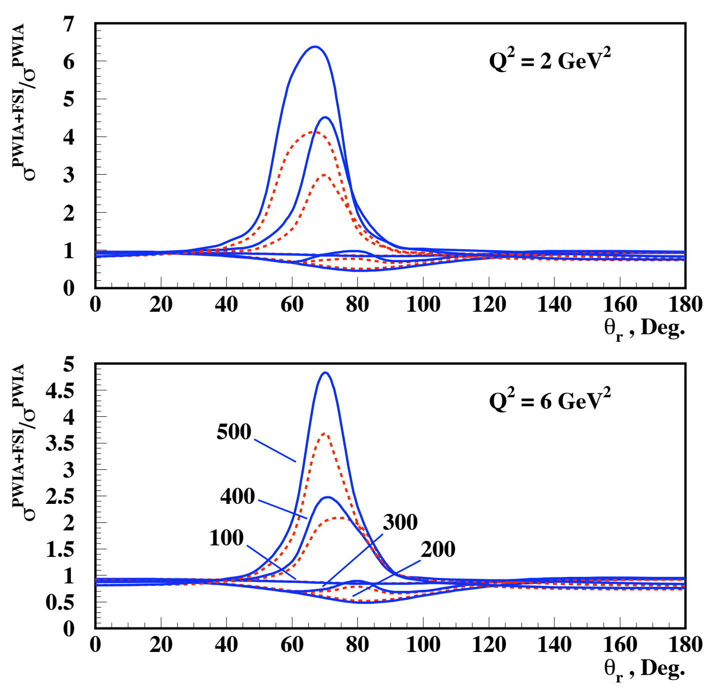

FIG. 3: Dependence of ratio R on the recoil angle of the neutron for different values of $p_r = 100, 200, 300, 400, 500$ MeV/c and $Q^2 = 2, 6$ GeV^2. Solid line - unfactorized and dashed line - factorized approximations.

A. Nonfactorization effects

In Fig.3 we compare the calculations of R with and without factorization approximation for the electromagnetic current in the FSI amplitude. The factorization approximation will result in the so called distorted wave impulse approximation (DWIA) widely used in the literature.

As the figure shows the factorization (or DWIA) approximation is applicable for up to $p_r \leq 300$ MeV/c or for the kinematics in which the FSI amplitude is smaller than the PWIA term. The factorization approximation breaks down in kinematics dominated by the rescattering process at $p_r \geq 400$ MeV/c. As the comparisons show, the unfactorization predicts a larger FSI amplitude which can be understood based on the fact that in this case the electromagnetic current which enters in the rescattering amplitude of Eq.(30) is defined at smaller values of bound nucleon momenta than the electromagnetic current in the PWIA term (Eq.(19)).

Fig.3 shows also that the factorization approximation is Q^2 dependent and somewhat improves with an increase of Q^2. This is a rather important feature which should be taken into account in color transparency studies (CT) for double scattering kinematics, in which case the Q^2 dependence of the peak of the ratio R is studied in order to extract the CT signal (see e.g [31, 62, 63]). Our comparisons in Fig.3 shows that the unfactorized approximation should be used as a baseline for identification of the CT signature in the Q^2 dependence of the FSI contribution of the deuteron break-up cross section.

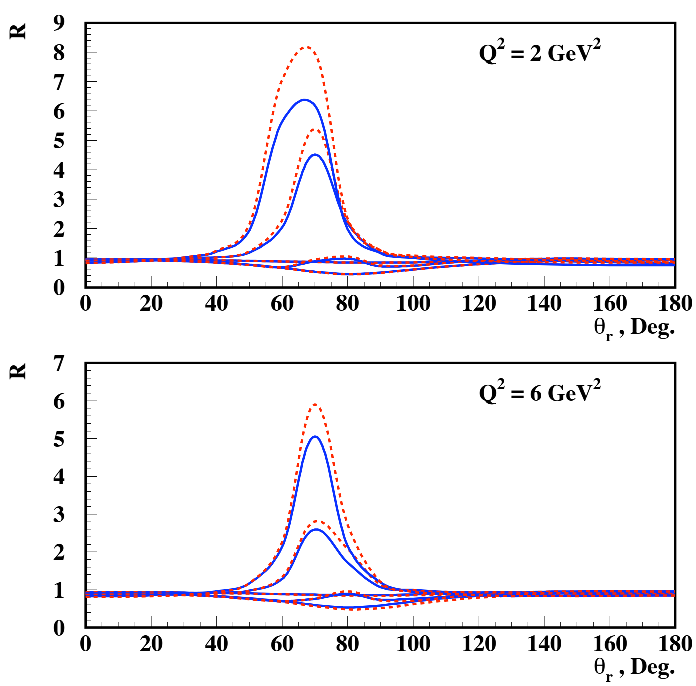

FIG. 4: Dependence of ratio R on the recoil angle of the neutron for different values of p_r and $Q^2 = 2, 6$ GeV^2. The recoil neutron momenta are the same as in Fig.3. Solid line - unfactorized calculation with the pole term only in the FSI amplitude, dashed line - unfactorized approximations with both pole and principal value terms in the FSI amplitude.

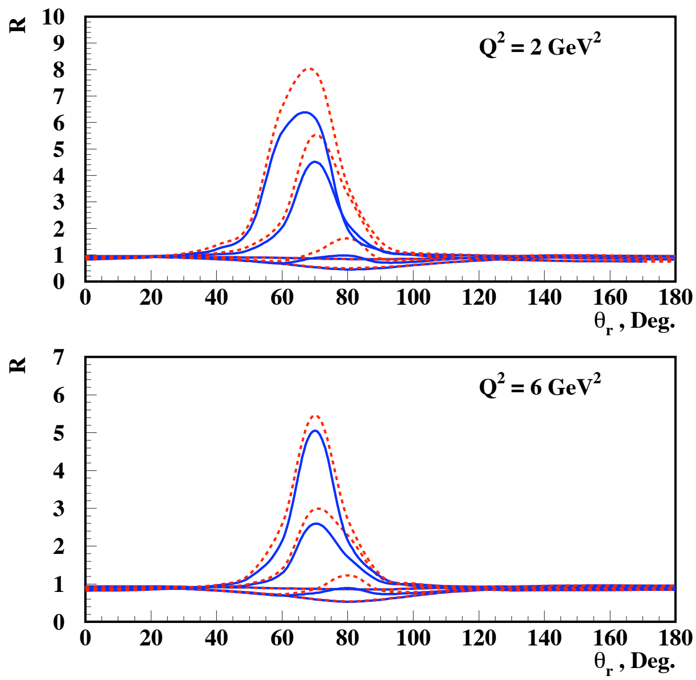

FIG. 5: Dependence of ratio R on the recoil angle of the neutron for different values of p_r and $Q^2 = 2, 6$ GeV^2. The recoil neutron momenta are the same as in Fig.3. Solid line - unfactorized approximation with the pole term only forward $pn \to pn$ rescattering, dashed line - unfactorized approximation including the pole terms for both forward $pn \to pn$ and charge-exchange $pn \to np$ rescattering amplitudes.

B. Off-Shell FSI Effects

Next we consider the contribution to the FSI amplitude due to the principal value part of Eq.(30). This term depends on the half-off shell NN scattering amplitude which is a largely unknown quantity. Therefore the reliability of our calculations depends on the magnitude of the principal value term. In Fig.4 we compare the calculations in which only the pole (on-shell) term of the FSI amplitude is included with the calculations which contain both pole (on-shell) and principal value (off-shell) terms of the FSI amplitude. For the half-off shell f_{pn} amplitude we use the approximation of Eq.(32). An important observation can be made from Fig.4 is that the off-shell rescattering effects diminish with an increase of Q^2. This is consistent with our earlier observation[11, 12] that the distances that the virtual nucleon propagates before the rescattering decreases significantly with an increase of Q^2 at fixed values of x.

C. Charge Exchange Rescattering Effects

Due to the fact that the charge-exchange rescattering amplitude is predominantly real it will interfere mainly with the real part of the forward elastic FSI amplitude which is a small

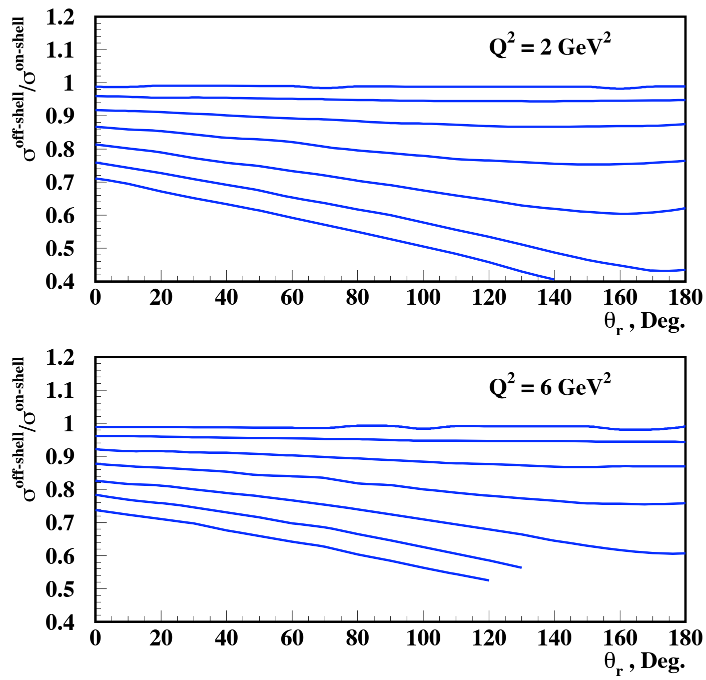

FIG. 6: Ratio of PWIA cross sections calculated using on-shell and off-shell approximations for the electromagnetic current of the proton. The curves from top to bottom correspond to recoil neutron momenta 100, 200, 300, 400, 500, 600 and 700 MeV/c respectively.

parameter at large energies. One can see from Fig.5 that the charge-exchange rescattering dominates at kinematics in which the rescattering defines the overall magnitude of the cross section.

However it is a rather well known fact that, due to the dominant pion-exchange nature of charge-exchange pn scattering, its cross section decreases linearly with an increase of the invariant energy s as compared to the forward pn elastic scattering cross section. As a result one expects that with an increase of Q^2 the charge exchange rescattering term will become a small correction. This can be seen from the calculation for $Q^2 = 6$ GeV^2 kinematics in Fig.5.

D. Off-Shell Electromagnetic Interaction Effects

The above evaluations of the $d(e, e'p)n$ cross sections demonstrate that in the large Q^2 limit the property of the scattering is defined mainly by the PWIA and forward angle on-shell FSI terms. The angular distribution has a very characteristic shape in which one can identify kinematics dominated by PWIA or FSI. Calculations also show that the forward or backward kinematics of the recoil nucleon are best suited for isolating PWIA term which subsequently allows us to study the structure of the electromagnetic current of the bound nucleon and the deuteron wave function at large values of internal momenta.

We now concentrate on the effects related to the fact that the proton in the deuteron becomes increasingly off-shell at large values of recoil neutron momenta in forward/backward

directions.

As it follows from Eqs.(15,18) and (20) the off-shell part of the electromagnetic current will diminish the overall magnitude of the electromagnetic interaction. Since the off-shellness grows with an increase of the initial momentum of the struck nucleon it will result in the suppression of the electromagnetic interaction strength of deeply bound nucleons. As it follows from Fig.6 the off-shell effects have a weak Q^2 dependences and to disentangle them from the effects related to the high momentum component of the deuteron wave function would require measurements covering an extended angular and recoil momentum range. Fig.6 also shows that the forward direction of recoil nucleon momenta represents the most optimal kinematic region for minimizing the off-shell effects for electromagnetic interaction.

Note that polarization measurements will provide additional observables for separating current and wave function effects. For example, measurements of the cross section asymmetries similar to Ref.[64] at large recoil momenta will be more sensitive to the structure of the electromagnetic current since wave function effects largely cancel out in the ratios defining the asymmetry.

E. Comparison with Experimental Data

In the last few years three experiments[25, 26, 27] produced first data at relatively large Q^2 kinematics.

The first experiment[25] probed the $Q^2 = 0.665$ GeV^2 and $x \approx 1$ kinematics and provided very accurate data. The measured value of Q^2 is marginal for the application of GEA. However as Fig.7 shows the comparison yields a surprisingly good agreement with the data. Fig.7 compares the reduced cross section defined as follows:

$$\sigma_{red} = \frac{d\sigma}{dE'_e, d\Omega_{e'} dp_f d\Omega_f} \cdot \frac{\mid \frac{p_f}{E_f} + \frac{p_f - q cos(\theta_{p_f,q})}{E_r} \mid}{\sigma_{CC1} \cdot p_f^2} \tag{50}$$

where the differential cross section is defined according to Eq.(45) and σ_{CC1} is the off-shell electron-proton cross section defined in Ref.[47]. Note that in this calculation for f_{pn} amplitude we use SAID[51] parameterization for both elastic and charge-exchange pn scatterings which fit the elastic pn scattering data for lab momenta up to 1.3 GeV/c. Because of the relatively low energy and momentum transfers involved in the reaction the calculation shows a substantial contribution from the off-shell as well as charge exchange parts of the FSI amplitude (difference between dotted, dash-dotted and solid lines in Fig.7).

It is worth noting that in agreement with the observations of Refs.[27, 38] the calculation overestimates the low recoil momentum part of the cross section (Fig.7b), where we expect that theoretical uncertainties are well under control. Our preliminary estimates demonstrate that this discrepancy could be accounted for by inclusion of the contribution of two-photon exchange effects in the overall amplitude of the scattering[65].

The second experiment[26]) covered the Q^2 range from $2-5$ GeV^2. However, due to the low statistics the data are integrated over the ranges of the recoil nucleon momenta.

Comparing with these data we performed the same kinematic integrations as the experiment did. The results are shown in Fig.8 and 9. Despite these integrations we still can make several important observations from these comparisons.

- First, the angular distribution clearly exhibits an eikonal feature, with the minimum (Fig.8) or maximum (Fig.9) at transverse kinematics due to the final state interaction.

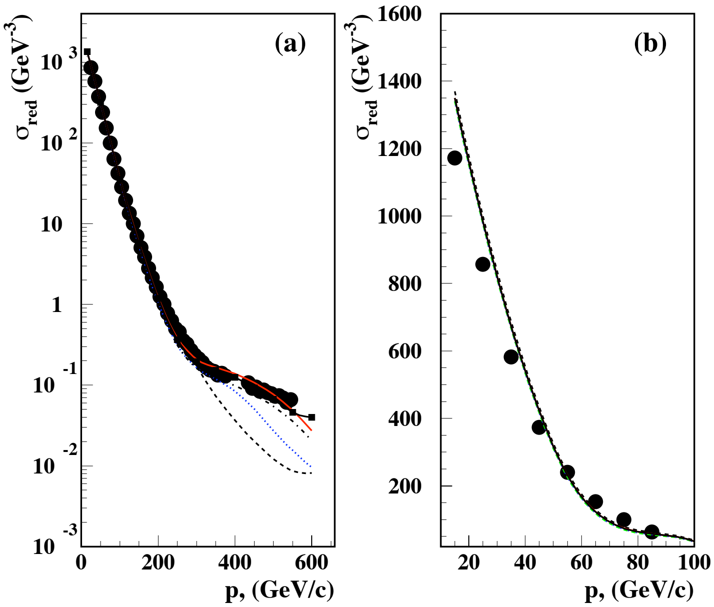

FIG. 7: Missing momentum dependence of the reduced cross section. The data are from Ref.[25]. Dashed line - PWIA calculation, dotted line - PWIA+ only pole term of forward FSI, dash-dotted line - PWIA+ forward FSI, solid line - PWIA + forward and charge exchange FSI, and solid line with squares - same as the previous solid line, added the contribution from the mechanism in which the proton is a spectator and the neutron was struck by the virtual photon.

The most important result is that the maximum of FSI is at recoil angles of 70^0 in agreement with the GEA prediction of Ref.[40]. Note that the conventional Glauber theory predicted 90^0 for the FSI maximum.

- The disagreement of the calculation with the data at $\theta_r > 70^0$ appears to be due to the isobar contribution at the intermediate state of the reaction. This region corresponds to $x < 1$ and it is kinematically closer to the threshold of Δ-isobar electroproduction. The comparisons also indicate that the relative strength of the Δ-isobar contribution diminishes with an increase of Q^2 and at neutron production angles $\theta_r \to 180^0$.

- The forward direction of the recoil nucleon momentum, being far from the Δ-isobar threshold, exhibits a relatively small contribution due to FSI. This indicates that the forward recoil angle region is best suited for studies of PWIA properties of the reaction such as the off-shell electromagnetic current and deuteron wave function.

Finally, the results of the experiment of Ref.[27] are currently in the final stages of analysis. Since in this experiment the disintegration reaction is measured at forward recoil angles and at Q^2 up to 3.5 GeV^2, we expect that it will allow us to further check the validity of our claim that the forward angular region is best suited for studies of the PWIA properties of the reaction.

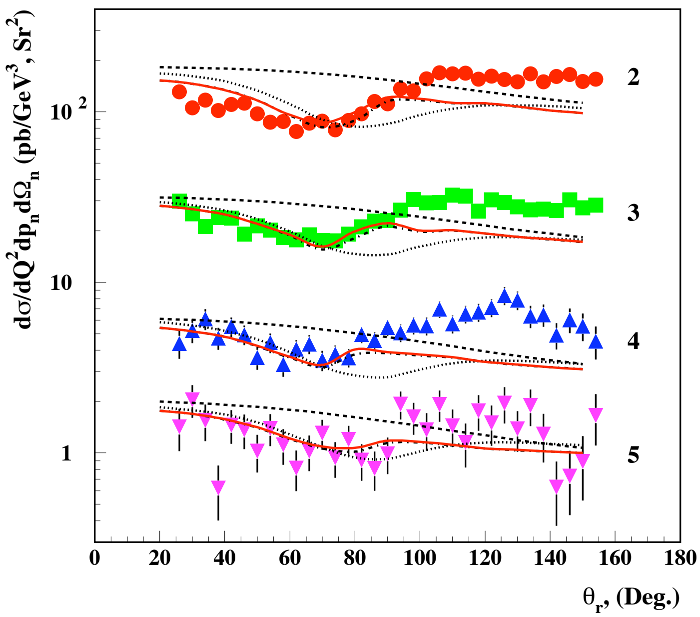

FIG. 8: Dependence of the differential cross section on the direction of the recoil neutron momentum. The data are from Ref.[26]. Dashed line - PWIA calculation, dotted line - PWIA+ pole term of forward FSI, dash-dotted line - PWIA+forward FSI, solid line - PWIA + forward and charge exchange FSI. The momentum of the recoil neutron is restricted to $200 < p_r < 300$ MeV/c. The labels 2, 3, 4 and 5 correspond to the following values of $Q^2 = 2 \pm 0.25; 3 \pm 0.5; 4 \pm 0.5; 5 \pm 0.5$ GeV^2.

IV. CONCLUSIONS

Within the virtual nucleon approximation we developed a theoretical framework for calculation of high Q^2 exclusive electrodisintegration of the deuteron at large values of recoil nucleon momenta. The scattering amplitude is derived based on generalized eikonal approximation, in which case each amplitude is calculated based on effective Feynman diagram rules. Because of the covariant formulation of the problem the electromagnetic current is gauge invariant from the beginning. By isolating the off-shell part in the electromagnetic current we introduced an approach which allows us to express the bound nucleon current separately through the on-shell and off shell parts.

Next, we derived the final state interaction amplitude based on GEA and expressed it through the on-shell and off-shell rescattering parts. No factorization approximation is assumed in the calculation of the FSI amplitude. The calculation of FSI also includes the amplitude due to the charge-exchange final state interaction.

We performed numerical analysis of the obtained formulae to identify the level of uncertainties due to the factors included in the calculations. Overall, our conclusion is that with an increase of Q^2 all the uncertainties related to the off-shell FSI and charge exchange rescattering became small and the total scattering amplitude is determined by the PWIA and on-shell elastic NN rescattering.

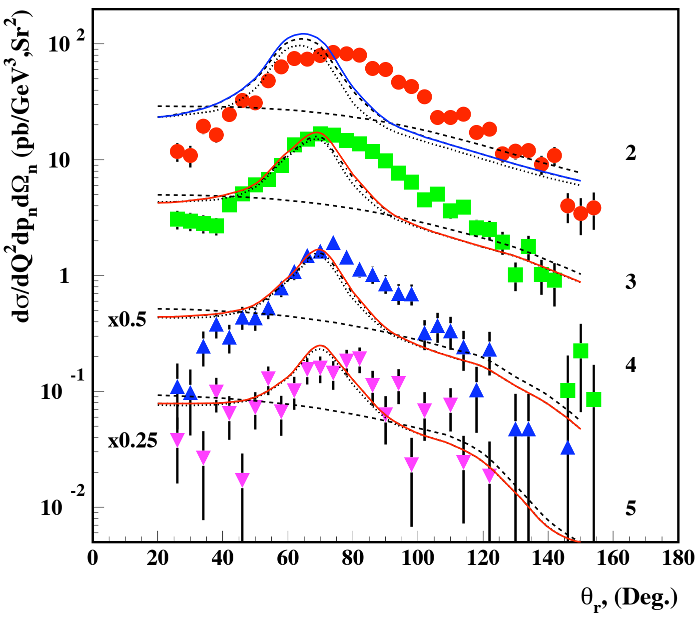

FIG. 9: Dependence of the differential cross section on the direction of the recoil neutron momentum. The data are from Ref.[26]. Dashed line - PWIA calculation, dotted line - PWIA+ pole term of forward FSI, dash-dotted line - PWIA+forward FSI, solid line - PWIA + forward and charge exchange FSI. The momentum of the recoil neutron is restricted to $400 < p_r < 600$ MeV/c. The labels 2, 3, 4 and 5 correspond to the following values of $Q^2 = 2\pm0.25; 3\pm0.5; 4\pm0.5; 5\pm0.5$ GeV^2. The data sets and calculations for "4" and "5" are multiplied by 0.5 and 0.25 respectively.

We compared our calculations with the first experimental data at large Q^2 deuteron electrodisintegration. These comparisons revealed a rather surprising agreement with low $Q^2 = 0.665$ GeV^2 data which indicates the wider range of applicability of the present approximation.

Comparisons with higher Q^2 data (≥ 2 GeV^2) at the wider range of recoil nucleon momenta and angles demonstrate the important role that the intermediate Δ-Isobar production plays in electrodisintegration reaction at backward angles close to the Δ production threshold.

However, at forward recoil angles where FSI effects are restricted, the calculations show greater sensitivity to the PWIA structure of the electrodisintegration reaction. Further experiments will allow us to confirm that this region is most suitable for probing the bound nucleon electromagnetic current and the deuteron wave function at small distances.

Acknowledgments

I'm thankful to Drs. Werner Boeglin, Mark Strikman and late Kim Egiyan for numerous discussions on the physics of deuteron break-up. I regret that this work was completed too late for Kim to see the importance of his deuteron break-up experiment. This work is

supported by the U.S. Department of Energy Grant under Contract DE-FG02-01ER41172.

---

[1] V. G. J. Stoks, R. A. M. Klomp, C. P. F. Terheggen and J. J. de Swart, Phys. Rev. C **49**, 2950 (1994).

[2] R. B. Wiringa, V. G. J. Stoks and R. Schiavilla, Phys. Rev. C **51**, 38 (1995).

[3] R. Machleidt,Phys. Rev. C **63**, 024001 (2001).

[4] M. Lacombe, B. Loiseau, J. M. Richard, R. Vinh Mau, J. Cote, P. Pires and R. De Tourreil, Phys. Rev. C **21**, 861 (1980).

[5] S. Sawada, "J-PARC, Japan Proton Accelerator Research Complex," Nucl. Phys. A **782**, 434 (2007).

[6] M. F. Lutz, B. Pire, O. Scholten and R. Timmermans [The PANDA Collaboration], "Physics Performance Report for PANDA: Strong Interaction Studies with Antiprotons," arXiv:0903.3905 [hep-ex].

[7] L. L. Frankfurt and M. I. Strikman, Phys. Rept. **76**, 215 (1981).

[8] L. L. Frankfurt and M. I. Strikman, Phys. Rept. **160**, 235 (1988).

[9] M. M. Sargsian *et al.*, J. Phys. G **29**, R1 (2003).

[10] M. M. Sargsian, Int. J. Mod. Phys. E **10**, 405 (2001).

[11] L. Frankfurt, M. Sargsian and M. Strikman, Int. J. Mod. Phys. A **23**, 2991 (2008).

[12] L. L. Frankfurt, M. I. Strikman, D. B. Day and M. Sargsian, Phys. Rev. C **48**, 2451 (1993).

[13] K. S. Egiyan *et al.* [CLAS Collaboration], Phys. Rev. C **68**, 014313 (2003).

[14] K. S. Egiyan *et al.* [CLAS Collaboration],Phys. Rev. Lett. **96**, 082501 (2006).

[15] R. Shneor *et al.* [Jefferson Lab Hall A Collaboration], Phys. Rev. Lett. **99**, 072501 (2007).

[16] R. Subedi *et al.*, Science **320**, 1476 (2008).

[17] Y. Mardor *et al.*, Phys. Lett. B **437**, 257 (1998).

[18] J. L. S. Aclander *et al.*, Phys. Lett. B **453**, 211 (1999).

[19] A. Tang *et al.*, Phys. Rev. Lett. **90**, 042301 (2003).

[20] I. Yaron, J. Alster, L. Frankfurt, E. Piasetzky, M. Sargsian and M. Strikman, Phys. Rev. C **66**, 024601 (2002).

[21] E. Piasetzky, M. Sargsian, L. Frankfurt, M. Strikman and J. W. Watson, Phys. Rev. Lett. **97**, 162504 (2006).

[22] M. M. Sargsian, T. V. Abrahamyan, M. I. Strikman and L. L. Frankfurt, 71, 044615 (2005).

[23] R. Schiavilla, R. B. Wiringa, S. C. Pieper and J. Carlson,Phys. Rev. Lett. **98**, 132501 (2007).

[24] M. Alvioli, C. Ciofi degli Atti and H. Morita, Phys. Rev. Lett. **100**, 162503 (2008).

[25] P. E. Ulmer *et al.*, Phys. Rev. Lett. **89**, 062301 (2002).

[26] K. S. Egiyan *et al.* [the CLAS Collaboration], Phys. Rev. Lett. **98**, 262502 (2007).

[27] W. U. Boeglin, Eur. Phys. J. A **24**, 77 (2005); L. Coman, " $^2H(e,e'p)$ Studies of the Deuteron at High Q^2", PhD. Thesis (*unpublished*), (2008).

[28] White Paper: "The Science Driving the 12 GeV Upgrade of CEBAF", Jefferson Lab, Newport News, VA, 2000.

[29] L. Frankfurt, E. Piasetsky, M. Sargsian and M. Strikman, Phys. Rev. C **51**, 890 (1995).

[30] A. Bianconi, S. Jeschonnek, N. N. Nikolaev and B. G. Zakharov, Phys. Lett. B **343**, 13 (1995).

[31] L. L. Frankfurt, W. R. Greenberg, G. A. Miller, M. M. Sargsian and M. I. Strikman, Z. Phys. A **352**, 97 (1995).

[32] L. L. Frankfurt, E. Piasetzky, M. M. Sargsian and M. I. Strikman,Phys. Rev. C **56**, 2752

(1997).
[33] S. Jeschonnek, Phys. Rev. C **63**, 034609 (2001).
[34] C. Ciofi degli Atti, L. P. Kaptari and D. Treleani, Phys. Rev. C **63**, 044601 (2001).
[35] C. Ciofi degli Atti and L. P. Kaptari, arXiv:nucl-th/0407024.
[36] J. M. Laget, Phys. Lett. B **609**, 49 (2005).
[37] S. Jeschonnek and J. W. Van Orden, Phys. Rev. C **78**, 014007 (2008).
[38] S. Jeschonnek and J. W. Van Orden, arXiv:0907.3712 [nucl-th].
[39] J.J. Adam, F. Gross, S. Jeschonnek, P. Ulmer and J. W. Van Orden, Phys. Rev. C **66**, 044003 (2002).
[40] L. L. Frankfurt, M. M. Sargsian and M. I. Strikman, Phys. Rev. C **56**, 1124 (1997).
[41] M. M. Sargsian, T. V. Abrahamyan, M. I. Strikman and L. L. Frankfurt, Phys. Rev. C **71**, 044614 (2005).
[42] C. Ciofi delgi Atti and L. P. Kaptari,Phys. Rev. Lett. **100**, 122301 (2008).
[43] M. Alvioli, C. Ciofi degli Atti and L. P. Kaptari, arXiv:0904.4045 [nucl-th].
[44] M. Sargsian, *in progress.*
[45] V. N. Gribov, J. Exp. Theor. Phys **30**, 709 (1970).
[46] L. Bertuchi, IL Nuovo Cimento A **11**, 45 (1972).
[47] L. De Forest, Nucl. Phys. A **392**, 232 (1983).
[48] S. J. Brodsky and G. P. Lepage, Phys. Rev. D **22**, 2157 (1980).
[49] P. Stoler, Phys. Rept. **226**, 103 (1993).
[50] M. Ungaro *et al.* [CLAS Collaboration], Phys. Rev. Lett. **97**, 112003 (2006).
[51] R. A. Arndt, W. J. Briscoe, I. I. Strakovsky and R. L. Workman, Phys. Rev. C **76**, 025209 (2007).
[52] J.J. Kelly, Phys. Rev. C **70**, 068202 (2004).
[53] R. A. Gilman and F. Gross, J. Phys. G **28**, R37 (2002).
[54] L .L. Frankfurt and M. I. Strikman, Phys. Lett. B **64**, 433, (1976); Phs. Lett. B **183** , 254 (1987).
[55] P. V. Landshoff and J .C. Polkinghorne, Phys. Rev. D **18**, 153 (1978).
[56] M. M. Sargsian, L. L. Frankfurt and M. I. Strikman, Z. Phys. A **335**, 431 (1990).
[57] C. Ciofi degli Atti and S. Liuti, Phys. Rev. C **41**, 1100 (1990).
[58] L. L. Frankfurt, G. A. Miller, M. M. Sargsian and M. I. Strikman, Phys. Rev. Lett. **84**, 3045 (2000).
[59] M. M. Sargsian, S. Simula and M. I. Strikman, Phys. Rev. C **66**, 024001 (2002).
[60] M. Sargsian and M. Strikman, Phys. Lett. B **639**, 223 (2006).
[61] W. R. Gibbs and B. Loiseau, Phys. Rev. C **50**, 2742 (1994).
[62] L. L. Frankfurt, W. R. Greenberg, G. A. Miller, M. M. Sargsian and M. I. Strikman, Phys. Lett. B **369**, 201 (1996).
[63] K. Egiian, L. Frankfurt, W. R. Greenberg, G. A. Miller, M. Sargsian and M. Strikman, Nucl. Phys. A **580**, 365 (1994).
[64] S. Strauch *et al.* [Jefferson Lab E93-049 Collaboration], Phys. Rev. Lett. **91**, 052301 (2003).
[65] M. Sargsian, *in progress.*
[66] The best hopes for the restart of the program of high energy baryonic experiments are associated with the upcoming projects of J-PARC, Japan[5] and GSI, Germany[6].
[67] In further discussion we neglect the difference between proton and neutron masses denoting them by m.